Solid-state Reactions between CVD-TiO_2 and $BaCO_3$

Yoko SUYAMA and Akio KATO

Department of Applied Chemistry, Faculty of Engineering, Kyushu University, Hakozaki, Fukuoka 812

(Received July 17, 1976)

The solid-state reactions between CVD-TiO_2 powders of anatase- and rutile-forms with various particle sizes and $BaCO_3$ were investigated in O_2 and CO_2. The reactivity of the TiO_2 powders and the apparent activation energy for the reaction were independent of the crystal type of TiO_2. The reactivity of the TiO_2 powders increased remarkably as the particle sizes grew smaller than 0.15 μm. When such fine CVD-TiO_2 powders were used, the reaction proceeded to completion at temperatures below 1000 °C in both O_2 and CO_2 and gave fine $BaTiO_3$ powders. The particles of $BaTiO_3$ produced appeared single-crystalline and kept a shape similar to that of the starting TiO_2 particle. The sizes of the $BaTiO_3$ particles were controlled by those of the starting TiO_2 and were independent of those of $BaCO_3$.

On the solid-state reactions between TiO_2 and $BaCO_3$, there have been several investigations concerning the effects of the particle size and crystal type of the starting TiO_2 powders on the reactivity.[1,2] In these studies, anatase-TiO_2 powders were produced by wet methods and rutile-TiO_2 powders were prepared by the calcination of anatase-TiO_2 at temperatures above 900 °C. The primary TiO_2-particles aggregated in the powders, especially in calcined rutile-TiO_2 powders. Therefore, it is questionable whether or not the observed reactivities truly represent the effect of the size or crystal type of the primary TiO_2-particles.

On the other hand, both the anatase and rutile-TiO_2 powders produced by vapor-phase reactions (CVD-TiO_2) are characterized by high purity, a very closely controlled particle-size distribution, and easy dispersion, and consist of single-crystalline particles. Therefore, the effects of the size and crystal type of TiO_2-particles on the reactivity are expected to be caught more exactly by using CVD-TiO_2 powders. The present authors have reported that CVD-TiO_2 powders prepared from the $TiCl_4$-O_2 system show a high reactivity in the reaction with $BaCO_3$ and that the resulting $BaTiO_3$ powders consist of particles with the shape of the starting TiO_2 particles.[3]

In the present investigation, in order to elucidate the effects of the crystal type and particle size of TiO_2-particles on the reactivity and the properties of $BaTiO_3$ powders produced, the solid-state reaction between TiO_2 and $BaCO_3$ was carried out by using CVD-TiO_2 powders obtained from the reaction systems of $TiCl_4$-O_2, $TiCl_4$-H_2O, $TiCl_4$-H_2O-H_2, and $TiCl_4$-H_2-CO_2.

Experimental

Materials. The titanium dioxide powders were prepared by vapor-phase reactions, as has been described previously.[4,5] Their properties and electron micrographs are shown in Table 1 and Fig. 1, respectively. The TiO_2 powders obtained from the $TiCl_4$-H_2O-H_2 system consist of nealy spherical or cubic particles smaller than 0.1 μm in size (Figs. 1 (a) and (b)). The TiO_2 powders obtained from the $TiCl_4$-H_2-CO_2 system consist of plate-like particles grown preferentially in the plane perpendicular to the c-axis[5] (Figs. 1 (c) and (e)). The TiO_2 powders obtained from the $TiCl_4$-O_2 system consist of square and plate-like or square-bipyramidal particles grown in the plane perpendicular to the c-axis (Figs. 1 (d) and (f)).

TABLE 1. REACTION SYSTEMS AND THE CHARACTERISTICS OF TiO_2 POWDERS

No.	Reaction system	$D_{50}(D_{10}—D_{90})$ (μ)[a]	S_{BET} (m^2/g)[b]	W_A (%)[c]
a-20	$TiCl_4$-H_2O-H_2	0.05 (0.03—0.07)	—	0
a-15	$TiCl_4$-H_2O-H_2	0.06 (0.04—0.08)	21	5
a-13	$TiCl_4$-H_2O	0.09 (0.05—0.12)	—	52
a-7	$TiCl_4$-H_2O-H_2	0.09 (0.06—0.11)	17	100
A-11	$TiCl_4$-O_2	0.18 (0.13—0.24)	—	100
A-1	$TiCl_4$-O_2	0.37 (0.24—0.46)	8	100
R-22	$TiCl_4$-H_2-CO_2	0.42 (0.29—0.54)	3	0
R-7	$TiCl_4$-H_2-CO_2	1.0 (0.67—1.3)	—	5
D-1	$TiCl_4$-O_2	1.5 (1.1 —1.9)	1	100

a) D_{50}, D_{10}, and D_{90} are the particle sizes at which the weight of particles reaches 50, 10, and 90% respectively on the cumulative weight % distribution curve. b) Specific surface area obtained by the BET method. c) Content of the anatase form.

GR-grade $BaCO_3$ was obtained from Wako Pure Chemical Ind., Ltd. (purity>99.7%).[6] The particles of the $BaCO_3$ powder are needle-like and 0.5—10 μm long. They showed no weight loss when heated to 1000 °C at 5.4 °C/min in O_2.

Solid-state Reactions. Equimolar mixtures of TiO_2 and $BaCO_3$ were prepared by mixing with an ultrasonic wave in absolute ethanol. The mixture of 70—130 mg was heated in a platinum vessel up to 950—1100 °C at 5.4 °C/min in a flow of CO_2-free O_2 or CO_2. The flow rate was about 130—150 ml/min (the I.D. of the reactor was 17 mm). The weight loss caused by the reaction was followed by means of an electrobalance.[7] X-Ray diffraction [Co$K\alpha$] and electron-microscopic analyses of the products were done in the course of the reaction.

Results and Discussion

Thermogravimetric Analysis of Reactions between TiO_2 and $BaCO_3$. The TG curves of equimolar TiO_2-$BaCO_3$ mixtures are shown in Figs. 2 and 3. The reaction begins at about 530 °C, and the weight loss reaches 100% at 930—1010 °C in O_2. As the TiO_2 powders become finer, the reaction proceeds faster and the weight loss reaches 100% at a lower temperature; that is, the reactivity of the TiO_2 powders increases. The decrease in reactivity with the particle size of TiO_2, however, becomes smaller as the particles grow larger. In CO_2, the beginning and completion temperatures of the reaction are higher by 50 to 100 °C than those in

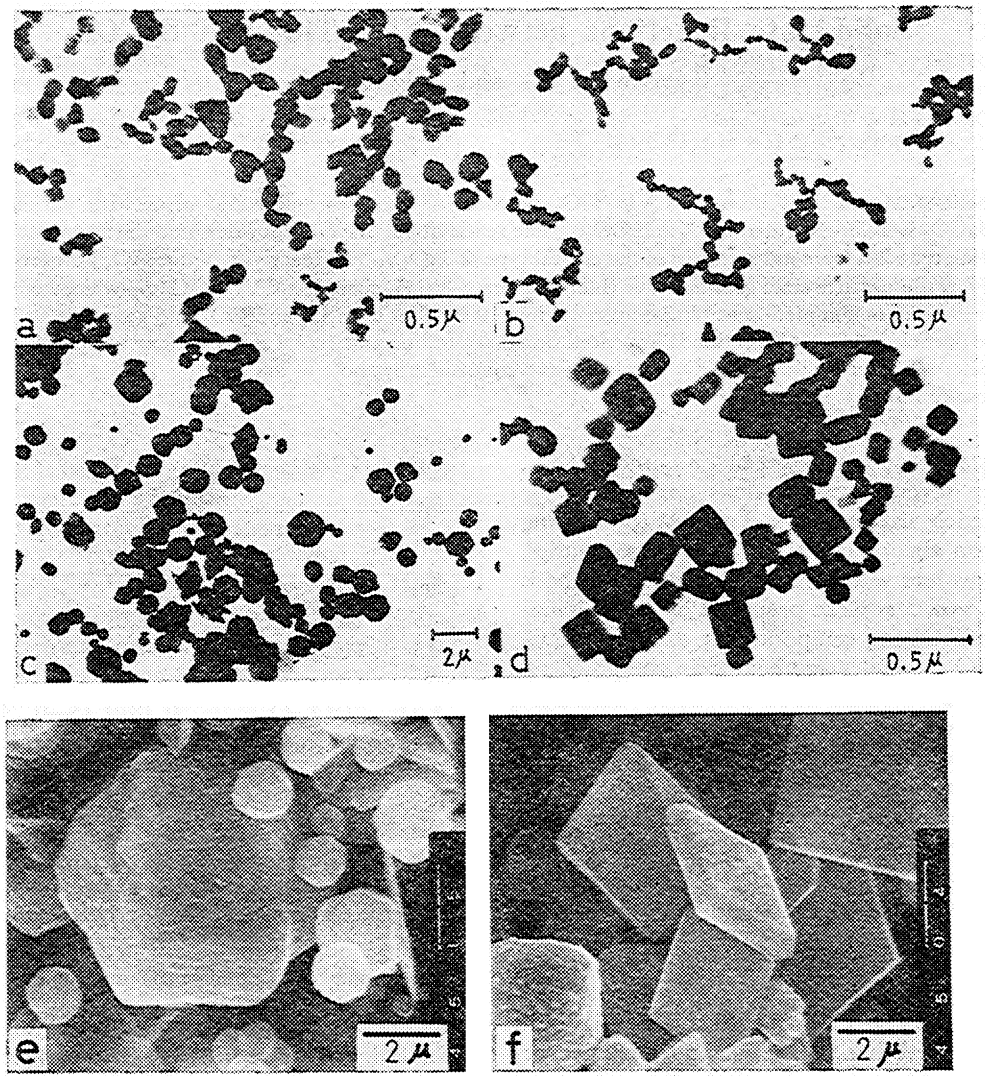

Fig. 1. Electron micrographs of TiO_2 powders.
(a), a-7; (b), a-15; (c) and (e), R-7; (d), A-11; (f), D-1.

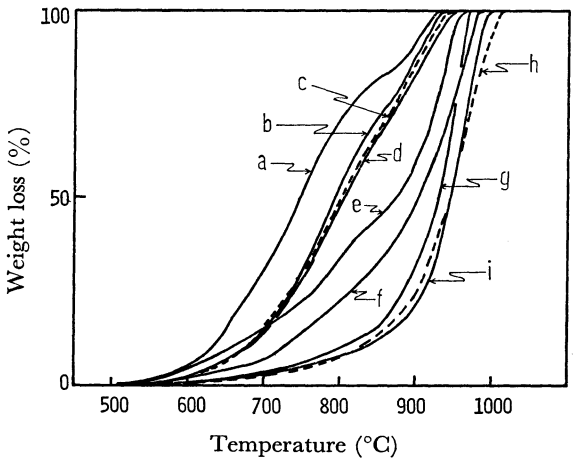

Fig. 2. TG curves of the reaction between TiO_2 and $BaCO_3$ in O_2.
TiO_2: (a), a-20; (b), a-15; (c), a-13; (d), a-7; (e), A-11; (f), R-22; (g), A-1; (h), R-7; (i), D-1.

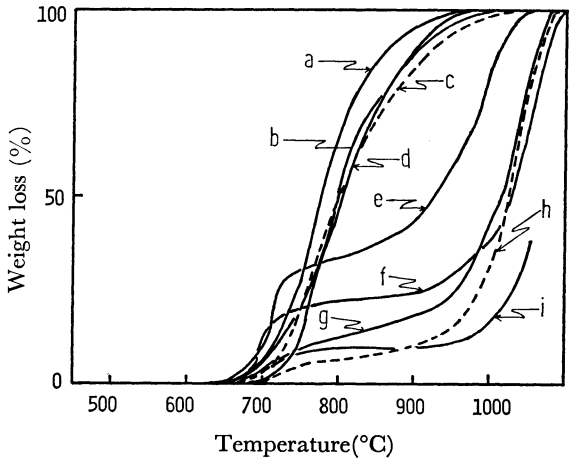

Fig. 3. TG curves of the reaction between TiO_2 and $BaCO_3$ in CO_2. Keys are the same as in Fig. 2.

O_2. The TG curves in CO_2 are classified into one- and two-step types. When the starting TiO_2 powders consist of particles smaller than 0.15 μm, the TG curves are of the first type and the reaction is completed below 1000 °C. When the TiO_2 powders contain particles larger than 0.15 μm, the TG curves are of the second type and the reaction is completed above 1000 °C. In the latter case, the rate of reaction in the first step is higher as the TiO_2 powders become richer in small particles. The difference in the TG curves between the reactions in O_2 and in CO_2 is due to the difference in the structure of the product layers.[3)]

In the reactions using other $BaCO_3$ powders which consisted of spherical particles finer than the present one,[3)] the TG curves changed with the particle size of TiO_2 in a manner similar to the present results, although the beginning and completion temperatures of the reaction were lower by 50—100 °C than in the present work. Therefore, the features of the TG curves in Figs. 2 and 3 may be considered to reflect the properties of the TiO_2 powders themselves.

The TG curves of a-15, a-13, and a-7, in which the

Table 2. Reaction products and activation energies for reactions in O_2

Group of TiO_2[a)]	Run	Former stage of reaction		Later stage of reaction	
		<850 °C Product[b)]	<840 °C E_a/kcal·mol^{-1}	>850 °C Product[b)]	>840 °C E_a/kcal·mol^{-1}
S	a-20	BT	55	BT	
	a-15	BT	56	BT	
	a-13	BT	56	BT	
	a-7	BT	56	BT	
L	A-11	BT	32	BT+B_2T	100
	R-22	BT	38	BT+B_2T	86
	A-1	BT	37	BT+B_2T	95
	R-7	BT	36	BT+B_2T	100
	D-1	BT	36	BT+B_2T	120

a) S, particle size <0.15 μm; L, the curves of the particle-size distributions extended above 0.15 μm.
b) BT, $BaTiO_3$; B_2T, Ba_2TiO_4.

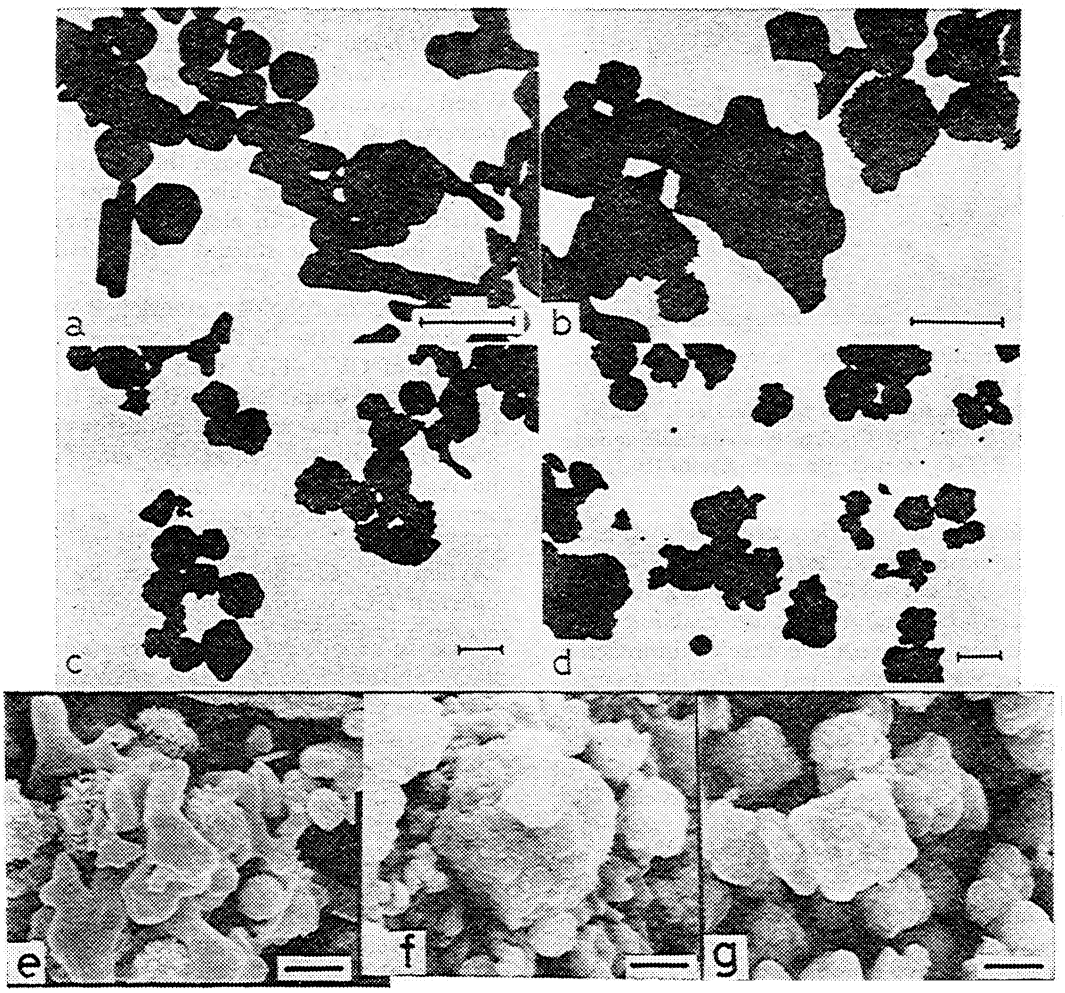

Fig. 4. Electron micrographs of the reaction products. (a), (b), (c), (d), (e), and (f), TiO_2: R-7, in O_2. Final temperature and % of reaction: (a), original mixture; (b) and (e), 905 °C, 25%; (c), 950 °C, 60%; (d) and (f), 1010 °C, 100%. (g), TiO_2: D-1, in O_2, 1062 °C, 100%. bar=2 μm.

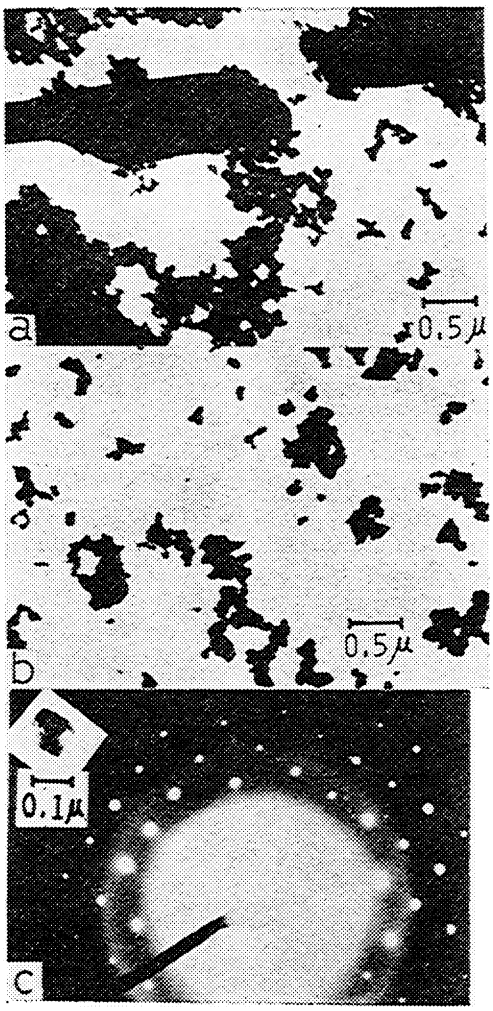

Fig. 5. Electron micrographs of the reaction products (TiO_2: a-15, in O_2).
Final temperature and % of reaction: (a), 780 °C, 50%; (b), 970 °C, 100%; (c), electron diffraction pattern of a $BaTiO_3$ particle shown in photo (b).

particle sizes of the TiO_2 powders are close, while the contents of the anatase-form differ, show little difference, indicating that the crystal form of TiO_2, whether anatase or rutile, does not affect the reactivity. It should be noted here that, in the course of the reaction of a-7, the unreacted TiO_2 consisted only of the anatase-form at 780 °C (the fraction reacted was 40%), although the anatase-rutile transition of the TiO_2 powders becomes appreciable above 900 °C when they are heated at 5.4 °C/min and the transition rate increases as the TiO_2 powders become finer.[3]

Reaction Products. The reaction products in O_2 are shown in Table 2, where the starting TiO_2 powders are classified into two groups according to the particle size: the TiO_2 powders consisting of particles smaller than 0.15 μm (S group) and the other TiO_2 powders (L group). In the S group, $BaTiO_3$ was the only product throughout the course of the reaction in both O_2 and CO_2. In the L group, $BaTiO_3$ was formed at first, and subsequently Ba_2TiO_4 was formed above 850 °C in O_2. The amount of Ba_2TiO_4 produced increased as the TiO_2 powders became coarser, in accord with the findings of a previous work.[1] In CO_2, the formation of Ba_2TiO_4 is suppressed thermodynamically up to 1145 °C.[8,9]

It is clear that the CVD-TiO_2 powders consisting of particles smaller than 0.15 μm show especially high reactivities and are converted into the $BaTiO_3$ powders at temperatures below 1000 °C.

Morphology of the Products. The electron micrographs of the products are shown in Figs. 4 and 5. Figure 4(a) shows the starting mixture of R-7. The particles of $BaCO_3$ are needle-like in shape. When a mixture is heated to 905 °C in O_2, products are formed on the surface of the TiO_2 particles consuming the neighboring $BaCO_3$ particles (Figs. 4(b) and (e)). The $BaCO_3$ particles become thinner with the progress of the reaction. When the mixture is finally heated to 1010 °C, all particles of the products maintain the outline of the starting TiO_2 particles (Figs. 4(d) and (f)). Figure 4(g) also shows the characteristic shape of the square and plate-like particles of the product in D-1 (compare with Fig. 1(f)). The change in the shape of particles in the course of the reaction of a-15 in O_2 is shown in Fig. 5. In this case, the change in the $BaCO_3$ particles is more significant. When the mixture is heated to 780 °C, large numbers of fine particles are attached to large particles of $BaCO_3$, as seen in Fig. 5(a). When the mixture is heated to 970 °C and wholly converted to $BaTiO_3$, the large particles disappear, as seen in Fig. 5(b). Although the particles are aggregated in part, they are cube-like and show the single-crystal pattern of $BaTiO_3$ in electron diffraction, the outline of the shape of the starting TiO_2 particles being held, too (Fig. 5(c)).

From the morphology mentioned above, it may be concluded that the $BaTiO_3$ is formed by a topotactical reaction of CVD-TiO_2 with $BaCO_3$. The manner of change in the shapes of the TiO_2 and $BaCO_3$ particles in the course of the reaction indicates that the reaction proceeds from the surface of the TiO_2-particle into the inside by the diffusion of the BaO component, forming a reaction-product layer on the surface of the TiO_2 particle.

When the reaction takes place by this model on a spherical TiO_2 particle with the radius of r_0, the fraction reacted α is given by:

$$\alpha = 1 - \left(\frac{r_0 - x}{r_0}\right)^3, \qquad (1)$$

where x is the thickness reacted. The values of α at 840 °C in Fig. 2, where $BaTiO_3$ is the only product, are compared in Fig. 6 with the ones calculated by means of Eq. 1. When the value of x at a given temperature is independent of r_0, the experimental and calculated values of α should agree. The agreement is not very good, but one can see that the present reaction model explains well the accelerated increase in the reactivity as the particle size of TiO_2 becomes smaller.

The particle-size distributions of the resulting $BaTiO_3$ and the starting TiO_2 are compared in Fig. 7. The average particle-size of the resulting $BaTiO_3$ is about 1.3 times that of the starting TiO_2. It is found that the TiO_2 powders with average particle-size of 1.3 μm were converted into the $BaTiO_3$ powders with that of

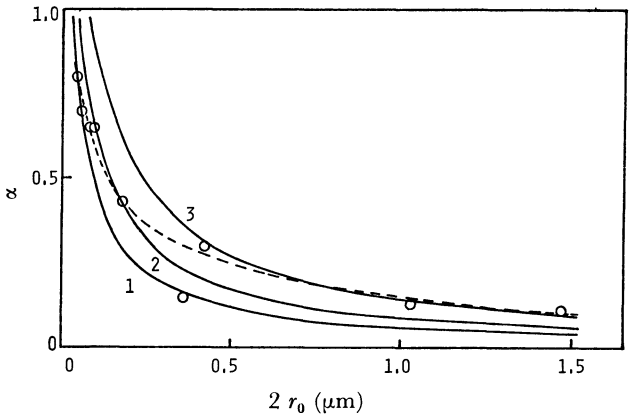

Fig. 6. Relation between the fraction reacted and particle size.
———, Calculated: 1, x=0.01 μm; 2, x=0.015 μm; 3, x=0.025 μm;
---○---, observed (at 840 °C).

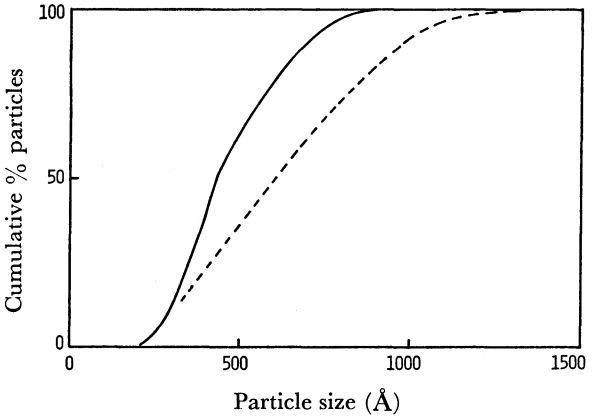

Fig. 7. Particle size distributions of the starting TiO_2 and the resulting $BaTiO_3$ powders of a-15.
——, TiO_2; ----, $BaTiO_3$.

1.6 μm,[3] the ratio of the average particle sizes being 1.2. When a TiO_2 particle is converted into a $BaTiO_3$ particle, the particle size should increase by 1.26 times. The observed values are close to the calculated one. This supports also the reaction model mentioned above.

When reaction mixtures are heated up to 1100 °C, the resulting $BaTiO_3$ particles suffer sintering to a considerable extent. However, the reaction can be completed below 1000 °C by selecting appropriate reaction conditions such as the particle size of TiO_2 and $BaCO_3$, the heating rate, or the atmosphere. In this case, the particle sizes of the $BaTiO_3$ powders produced are controlled by those of the starting TiO_2 powders, and one can produce ultrafine $BaTiO_3$ powders, which have a fineness comparable with that obtained by the thermal decomposition of oxalate,[11] by a solid-state reaction.

Application of Jander's Equation. When the reaction between TiO_2 and $BaCO_3$ powders occurs in the manner mentioned above, the reaction rate may be controlled by the diffusion of the BaO component through the product layer and the kinetics may follow Jander's equation (2):

$$(1-\sqrt[3]{1-\alpha})^2 = \frac{kt}{r_0^2} \quad (2)$$

where α is the fraction reacted at time t, k is the rate constant, and r_0 is the initial radius of the TiO_2 particle. We tried to analyze the TG curves in O_2 by the use of Jander's equation. To apply the equation to the TG data, it was modified as Eq. 3.[12-14]

$$K = \frac{2(1-\sqrt[3]{1-\alpha})}{3(1-\alpha)^{2/3}} \cdot \frac{\Delta\alpha}{\Delta T} = \frac{k_0}{ar_0^2} e^{-E/RT}, \quad (3)$$

where a is the heating rate. The values of K were calculated by taking ΔT=25 °C. Plots of log K *vs.* $1/T$ are shown in Fig. 8. Jander's equation holds well up to ≈770 °C for the S group and up to ≈840 °C for the L group. On the L group, the slope changes at ≈840 °C, suggesting that the reaction mechanism changes at this temperature. This may be caused by the appearance of Ba_2TiO_4 at ≈850 °C.

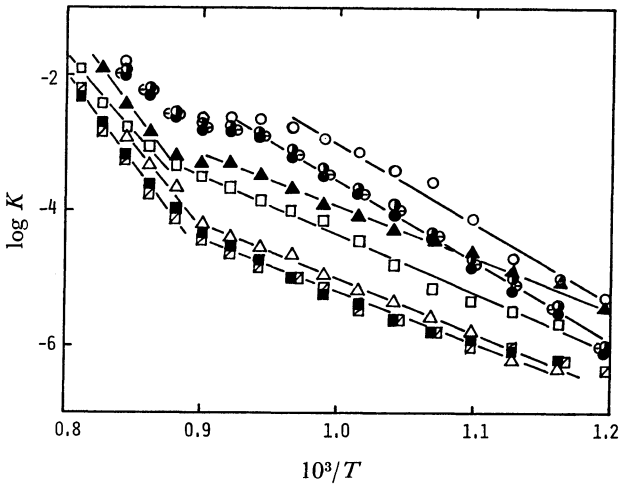

Fig. 8. Plots of log K *vs.* $10^3/T$ for the reactions in O_2.
○, a-20; ●, a-7; ◑, a-15; ⊖, a-13; △, A-1; ▲, A-11; □, R-22; ■, R-7; ▨, D-1.

From the linear parts of the plots, the apparent activation energies are obtained (see Table 2). The activation energies for the former stage are different between the S and L groups. However, it should be noted that the activation energy is also independent of the crystal type of TiO_2 in each group. The activation energies reported hitherto are shown in Table 3. All of these activation energies are claimed for the diffusion process. When the diffusion of the BaO component in the $BaTiO_3$ layer is the rate-determining step, each experiment should give comparable activation energies independently of the crystal type of TiO_2. This is not the case, as may be seen in Table 3. However, it is interesting to note that, regardless of the crystal type of TiO_2, most of the values fall into two ranges: 34—36 and 54—60 kcal/mol; this is in good agreement with the results of the present work. The value of 99 kcal/mol is close to that of the L group in the higher-temperature range in the present work. This exceptionally high value, therefore, is considered to be due to the formation of Ba_2TiO_4 and not to the fact that TiO_2 has a rutile form.

Table 3. Activation energy for the formation of $BaTiO_3$

Workers	Crystal type of TiO_2	E_a kcal·mol^{-1}	Rate equation
Kubo and Shinriki[16]	Anatase	54	Jander
Kubo and Shinriki[15]	Rutile	99	modified
	Anatase	58	Jander
Kuno *et al.*[2]	Rutile	36	Tamman
	Anatase	34	
Arai *et al.*[14]	Anatase	60	Jander

The reason why the activation energies differ between the S and L groups, although both groups give the same reaction product, $BaTiO_3$, below 840 °C, is not clear at present. However, the following should be noted here.

It has been reported by Nakayama and Sasaki[10] that the activation energy of the diffusion of barium into the rutile-TiO_2 crystal is 59 kcal/mol for a direction perpendicular to the c-axis and 43 kcal/mol for a direction parallel to the c-axis. The activation energies obtained for the S and L groups in the lower-temperature range are of the same order of magnitude as the values of the former and the latter, respectively. The rutile-TiO_2 particles used in the present work are spherical or cubic in the S group and plate-like grown in the plane perpendicular to the c-axis in the L group. Accordingly, in the reaction of the L group, the diffusion of the BaO component may mainly occur along the direction of the c-axis of rutile-TiO_2 and give a lower activation energy. On the other hand, in the reaction of the S group, the diffusion may occur more isotropically and give a higher activation energy. On anatase-TiO_2 particles, the same interpretation may be applied in explaining the different behavior between the two groups.

Reactivity and Crystal Type of TiO_2. On the solid-state reaction of the TiO_2–$BaCO_3$ system, it has generally been accepted that anatase-TiO_2 shows a lower activation energy and a higher reactivity than rutile-TiO_2.[1] In the present study, however, there were no observable differences in the reactivity and activation energy between anatase- and rutile-forms. This is to be expected when the reaction is limited by a diffusion through the same reaction product. The particle size of TiO_2 governs the reactivity. In previous works, in which the differences in the reactivity and the activation energy between the two forms of TiO_2 were observed, the secondary properties of the TiO_2 powders such as the state of the agglomeration of primary particles, especially in the case of calcined rutile-TiO_2, would affect the reactivity and result in different reactivities between the two types of TiO_2.

This research was supported in part by the Science Foundation of the Ministry of Education (No. 885150).

References

1) For example, T. Kubo, M. Kato, and T. Fujita, *Kogyo Kagaku Zasshi*, **70**, 847 (1967).
2) H. Kuno, A. Suzuki, and M. Yokoyama, *Funtai Oyobi Funmatsu Yakin*, **13**, 47 (1966).
3) Y. Suyama and A. Kato, *Ceramurgia Intern.*, **1**, 5 (1975).
4) Y. Suyama and A. Kato, *J. Am. Ceram. Soc.*, **59**, 146 (1976).
5) Y. Suyama, K. Ohmura, and A. Kato, *Nippon Kagaku Kaishi*, **1976**, 584.
6) Impurities; chloride<0.002%, heavy metals<0.001%, iron<0.001%, calcium and alkalies<0.25%, sulphide<0.001%.
7) Cahn RG electrobalance.
8) L. K. Templeton and J. A. Pask, *J. Am. Ceram. Soc.*, **42**, 212 (1959).
9) Y. Suyama and A. Kato, *Ceramurgia Intern.*, **1**, 123 (1975).
10) T. Nakayama and T. Sasaki, *Bull. Chem. Soc. Jpn.*, **36**, 569 (1963).
11) K. Kiss, J. Magder, M. S. Vukasovich, and R. J. Lockhart, *J. Am. Ceram. Soc.*, **49**, 291 (1966).
12) T. Kubo, S. Sirasaki, and M. Kato, *Kogyo Kagaku Zasshi*, **69**, 357 (1966).
13) A. Kato and Y. Suyama, *J. Therm. Anal.*, **7**, 149 (1975).
14) Y. Arai, T. Yasue, H. Takiguchi, and T. Kubo, *Nippon Kagaku Kaishi*, **1974**, 1611.
15) T. Kubo and K. Shinriki, *Kogyo Kagaku Zasshi*, **57**, 619 (1954).
16) T. Kubo and K. Shinriki, *Kogyo Kagaku Zasshi*, **55**, 49 (1952).